Available online at www.sciencedirect.com

SciVerse ScienceDirect

www.elsevier.com/locate/matchar

Variant selection of bainite on the surface of allotriomorphic ferrite in a low carbon steel

Hui Guo[a,*], *Xiangxi Gao*[a,b], *Yin Bai*[a], *Masato Enomoto*[c], *Shanwu Yang*[a], *Xinlai He*[a]

[a]*Department of Materials Physics and Chemistry, University of Science and Technology Beijing, Beijing 100083, PR China*
[b]*Laboratory on NDT, AVIC Beijing Institute of Aeronautical Materials, Beijing 100095, PR China*
[c]*Department of Materials Science and Engineering, Ibaraki University, Hitachi 316-8511, Japan*

ARTICLE DATA

Article history:
Received 29 November 2011
Received in revised form
6 February 2012
Accepted 8 February 2012

Keywords:
Steel
EBSD
Phase transformations
Bainite
Allotriomorphic ferrite

ABSTRACT

The crystallographic orientations of bainitic plates on the surface of allotriomorphic ferrite were analyzed in a low carbon Fe-0.05C-2.9Mn-1.8Si alloy which after austenitization was isothermally held successively at 725 and 340 °C. Nearly 80% of ferrite allotriomorphs had a Kurdjumov–Sachs orientation relationship with one of the austenite grains. In the grain that had an almost exact Kurdjumov–Sachs relationship with the ferrite allotriomorph bainitic plates nucleated with the same variant as that of ferrite. In the grain deviated slightly from the Kurdjumov–Sachs relationship bainitic plates chose the variant proximate to that of ferrite. No variant selection appeared to occur at irrational ferrite/austenite boundaries. The nucleation potency of Kurdjumov–Sachs related and irrational boundaries is discussed in terms of the ability of the variant of bainite nuclei to form a low energy boundary with the ferrite and the possible difference in the amount of carbon build-up which arises out of the difference in boundary mobility.

1. Introduction

The bainite microstructure is widely used in high performance steels due to its good mechanical property. Since the reduction in packet or block size of bainitic microstructure would improve both strength and toughness, the nucleation and variant selection of bainitic plates is gaining increasing attention [1–3]. Recent studies in medium carbon steels revealed that the misorientation between matrix austenite grains have a large influence on the variant selection of bainite [4,5].

To improve the weldability of high performance structural steels, the carbon content has to be reduced to a low level. In such steels allotriomorphic ferrite is formed at higher temperatures during cooling and a large proportion of prior austenite grain boundaries are replaced by the ferrite/austenite boundaries which serve as a preferred nucleation site of bainitic plates. Compared to nucleation of bainitic plates at austenite grain boundaries [4,6], nucleation at ferrite/austenite boundaries have not been fully studied. Quidort et al [7] observed in a 0.5%C steel that the formation of allotriomorphic ferrite eliminated the incubation time and stimulated the nucleation of bainite. Kim et al. [8] reported that bainite plates adjacent to the allotriomorphic ferrite had an orientation close to that of ferrite in an Fe–0.595C–0.98Si–1.10Mn–1.50Al steel. The detailed crystallographic analysis, however, is needed to evaluate correctly the nucleation potency of ferrite/austenite boundary and variant selection of bainitic plates thereat.

In low carbon steels one can not directly measure the orientation of austenite because very little amount of austenite is retained upon cooling. This problem has been solved recently; the orientation of a prior austenite grain can be determined from the distributions of poles of martensitic or bainitic plates [9,10]. In this report, the orientation relationship and variant selection of bainitic plates with the austenite grain and the allotriomorphic ferrite is analyzed using this

* *Corresponding author*. Tel.: +86 10 62334778; fax: +86 10 62332428.
E-mail address: guohui@mater.ustb.edu.cn (H. Guo).

1044-5803/$ – see front matter © 2012 Elsevier Inc. All rights reserved.
doi:10.1016/j.matchar.2012.02.009

technique and the potency of ferrite/austenite boundary as a nucleation site of bainite is discussed.

2. Experimental procedure

A high purity low carbon steel was melted in a vacuum induction furnace and cast into a 20 kg ingot, which was forged to 10 mm-thick plates and cut to 10×10×100 mm bars. The chemical composition of steel is: C 0.05, Mn 2.94, Si 1.78, P 0.01, S 0.009 (in wt.%). After homogenizing at 1300 °C for 48 h, they were cut to specimens, 7 mm in length and 10 mm in thickness, and were sealed in quartz tubes for heat treatment. The specimens were austenitized at 1250 °C for 1 h, cooled to 725 °C and isothermally held for 1 h. Then, they were cooled to 340 °C for 1 h and isothermally held for 1 h and quenched into water. After mechanical polishing the specimens were etched by 3% nital solution for optical microscopy. The specimen for EBSD analysis was electropolished in an alcoholic solution with 10% perchloric acid at ambient temperature for 30–40 s with the voltage of 20 V.

3. Results and discussion

3.1. *Microstructure obtained from two step isothermal holding*

Fig. 1 shows the microstructure of a specimen after two-step isothermal holding. The 1st isothermal holding temperature was close to the transition temperature from partitioned to no-partitioned growth of ferrite in this alloy [11]. Thus, ferrite allotriomorphs (bright areas) was formed presumably without partitioning of Mn or Si between ferrite and austenite. Bainitic microstructure was formed in the untransformed matrix during the 2nd isothermal holding. The M_s temperature of this alloy was calculated to be 428 °C from the equation proposed by Andrew [12]. For comparison the alloy was quenched into water immediately after holding at 725 °C. As shown in Fig. 2, the alloy was fully transformed into martensite. The

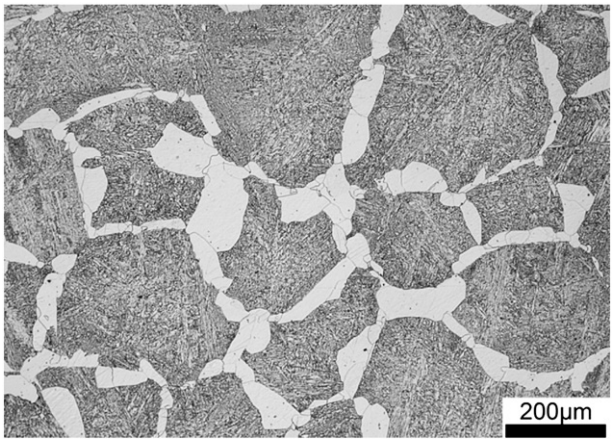

Fig. 1 – Micrograph of the sample isothermally held at 725 and 340 °C for 1 h after austenitized at 1250 °C for 1 h.

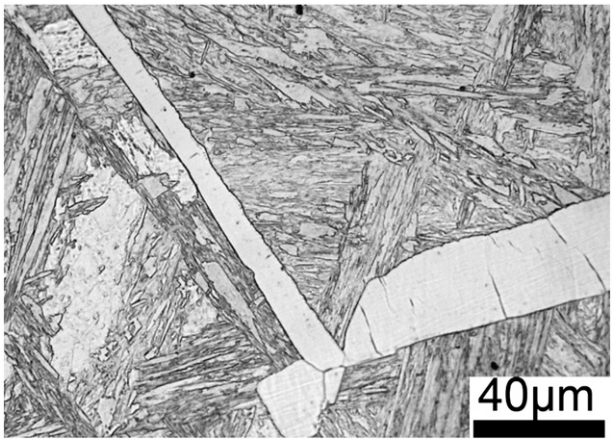

Fig. 2 – Micrograph of the sample isothermally held at 725 °C for 1 h followed by water quenching.

optical microscope observation showed that the interface between the martensite and adjacent ferrite is usually clear which suggests they are high-angle boundaries [13]. Some recent EBSD work further showed that compared with bainite, martensite less likely chooses the same variant with the adjacent grain boundary ferrite. The details will be described elsewhere [14]. As reported earlier [15], bainitic microstructure can be formed even below the M_s temperature in low and very low carbon steels. The variant selection of the bainite is different from that of martensite, as shown in the following section.

Fig. 3a shows a ferrite allotriomorph of which the phase boundary with the right austenite grain is clearly visible, and the phase boundary with the other austenite grain is not clearly delineated by etching. In contrast, the phase boundaries of an allotriomorph with the matrix are not clearly visible on either side in Fig. 3b. As previously noted [13,16], the thickness or visibility of boundaries after etching was correlated well with the existence of orientation relationship between ferrite allotriomorphs and the matrix. Indeed, King and Bell [17] reported more than a few decades ago that in an Fe-0.47C alloy grain boundary ferrite allotriomorphs had a fixed orientation relationship with at least one of the matrix grains, and a substantial proportion of ferrite allotriomorphs had the relationship with both grains. Similar observations have been made with bcc precipitates at fcc grain boundaries in other alloys [18–21]. In the present alloy nearly 80% of ferrite allotriomorphs were of the former type [13,16,22]. The average thickness of about 10% ferrite allotriomorphs of the latter type, having the orientation relationship on both sides, was 10.7 μm, while the average of all ferrite allotriomorphs was 31.5 μm [13]. These are consistent with a view that phase boundaries having a fixed orientation relationship are less mobile compared to those maintaining the orientation relationship proposed by Smith [23].

3.2. *Nucleation on ferrite allotriomorph K-S (K-S) oriented with one matrix grain*

The orientation map of the area in Fig. 3a is shown in Fig. 4a and b. The <001> poles of all bainitic plates in the left

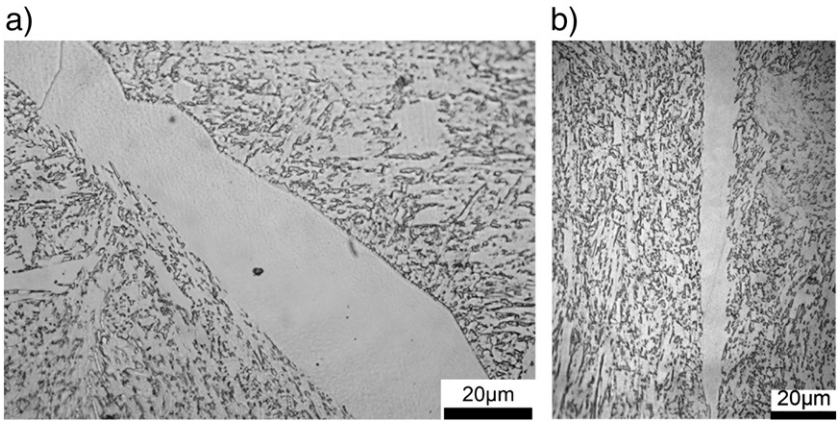

Fig. 3 – Micrograph of (a) an allotriomorphic ferrite with the ferrite/bainite interfaces clear on right side and unclear on left side and (b) one with the ferrite/bainite interface unclear on both sides.

austenite grain and in the right grain are given in Fig. 5a and c, respectively, together with the poles of 24 K-S variants calculated for each grain. It is seen that the matching between measured and calculated poles is good. This indicates that bainitic plates maintain a K-S relationship with the austenite grain in which they were formed.

In Fig. 5b and d the measured <001> poles of the ferrite allotriomorph are superposed on the poles of K-S variants. It is seen that the orientation of the ferrite allotriomorph is almost identical to variant 24 (denoted V24) associated with the left grain, while it does not appear to have an orientation relationship with the right grain. Readers are referred to ref. [24] for numbering the K-S variant. The deviation angle of the right austenite grain from the K-S relationship is calculated to be 22.5°.

As seen in Fig. 4a, a major fraction of the surface of the ferrite allotriomorph is covered by a thin plate of orange color. This plate was determined to be V24, the same as that of ferrite allotriomorph. This plate is in contact with another plate of green color on the other side, the variant being indexed as V21. The packet of bainitic plates usually consists of several blocks, each containing plates of a single variant. However, it was reported recently [3] that two variants with the smallest misorientation of 24 variants, i.e. 10.5°, formed a sub-block of bainite and shared the same habit plane with the matrix. V21 and V24 are the variants which can form a sub-block. Thus, a bainitic plate nucleates on the surface of ferrite allotriomorph with the same variant V24 as that of ferrite, grows to cover a major proportion of the ferrite/austenite boundary. The adjacent plate then chose variant V21 presumably to minimize strain energy, i.e. due to self-accommodation. Only a small part of ferrite/austenite boundary was covered by a plate of V21 with this allotriomorph.

In contrast, as seen in Fig. 4b, bainitic plates have many other variants in the right grain. A total of 11 variants are observed with plates in contact with the ferrite allotriomorph. It is difficult to judge whether these plates nucleated on the ferrite/austenite boundary or within the matrix and grew to impinge the ferrite. From the variants of these plates indexed in Fig. 4b, it seems that variant selection did not occur in this grain which did not possess a fixed orientation relationship with ferrite. Measured misorientation angles between the ferrite and bainitic plates are listed in Table 1. Indeed, they are all greater than 21°, thus forming a clear dark boundary upon etching.

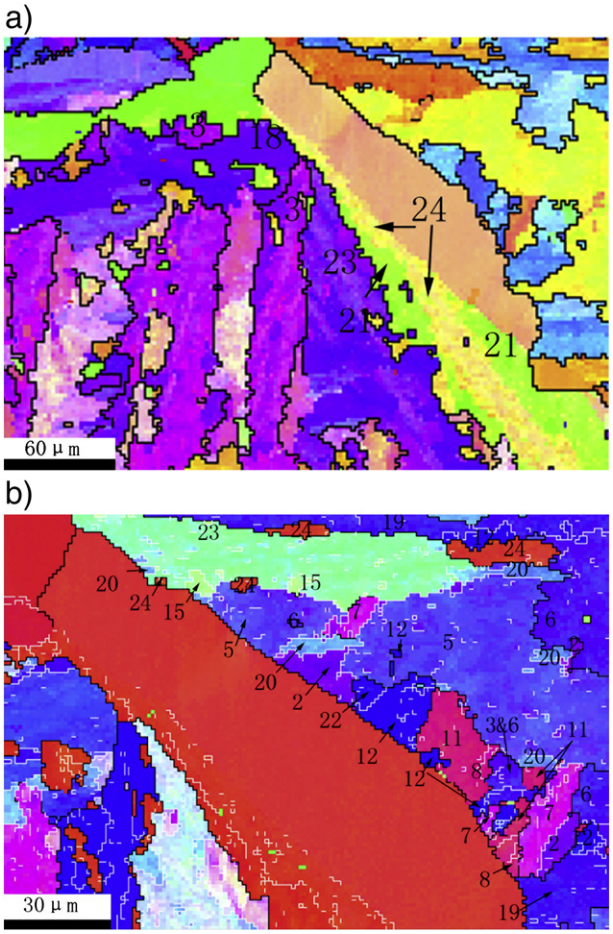

Fig. 4 – Inverse pole figures of the area in Fig. 3(a) for direction ND (a) and RD (b). ND and RD are directions perpendicular to each other, both of which are parallel to the sample surface.

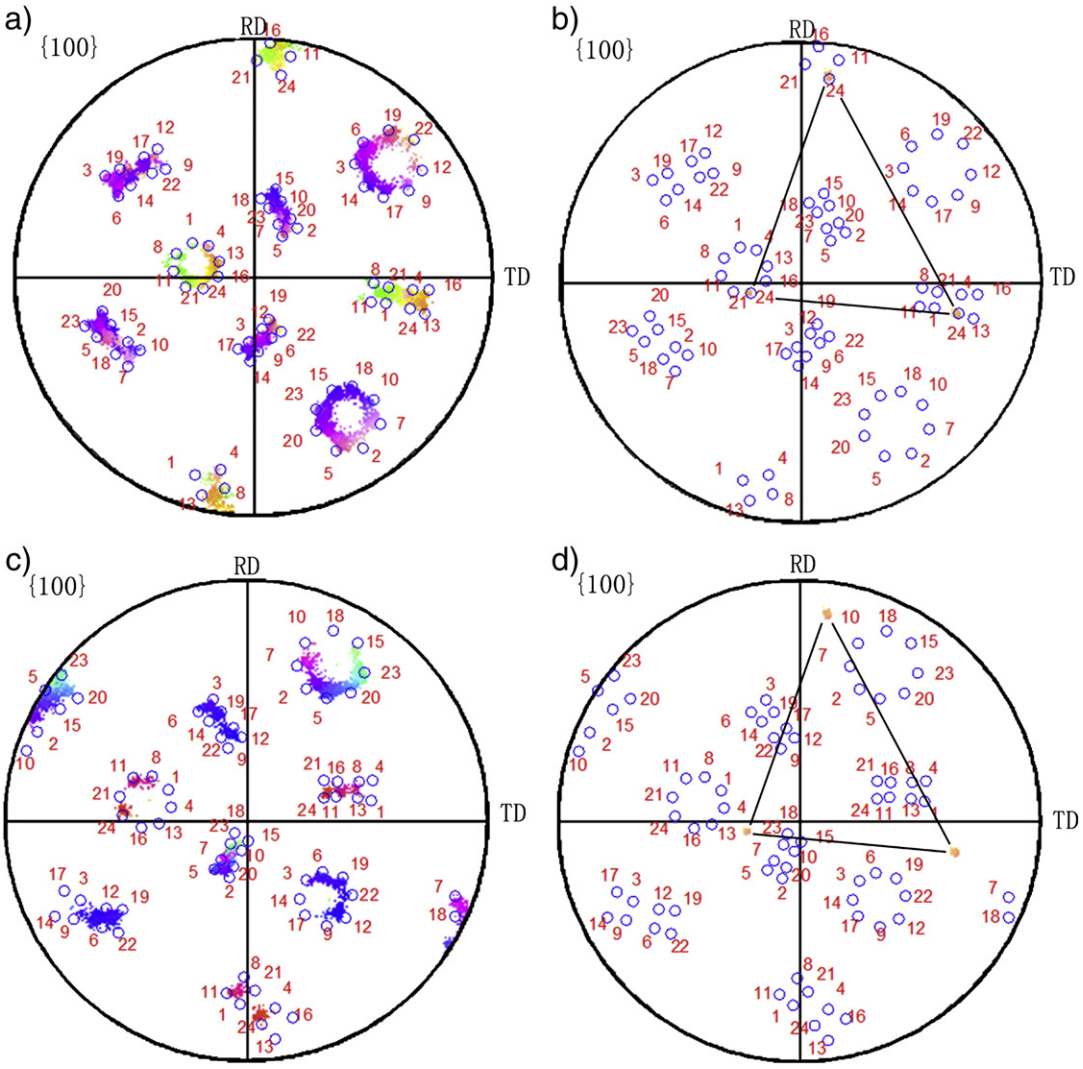

Fig. 5 – {100} pole figures of simulated K-S variants in the left grain of Fig. 4(a), superimposed by measured orientation of (a) bainite and (b) allotriomorphic ferrite; And {100} pole figures of simulated K-S variants in the right grain in Fig. 4(a), superimposed by measured orientation of (c) bainite and (d) allotriomorphic ferrite.

3.3. *Nucleation on ferrite allotriomorph K-S oriented with both matrix grains*

Fig. 6 shows an orientation map of the area surrounding the ferrite allotriomorph in Fig. 3b. The black dashed lines represent the position of ferrite/bainite boundaries. Measured <001> poles of bainite plates in left and right austenite grains are shown in Fig. 7a and c, respectively, in which calculated <001> poles of 24 K-S variants are superimposed on the measured data. It is clearly seen in these figures as well that bainitic plates maintain an almost exact K-S orientation relationship with the prior austenite grain.

The K-S variant of the ferrite allotriomorph with the left matrix grain was determined to be V2 by comparing with the calculated pole figure, as shown in Fig. 7b. The variant of bainitic plate immediately adjacent to the ferrite was also V2, and this plate is in contact with the ferrite along the whole surface. It is noted that small plates of V5, forming a sub-block with V2, are observed in this region. On the other hand, the right grain deviated 5.2° from the exact K-S relationship with the ferrite. The orientations of bainitic plates in contact with the ferrite are V9, V12 and V17 and none of them coincide exactly with the orientation of ferrite as in the left grain. Indeed, these variants deviated from the ferrite by 8, 3

Table 1 – Measured misorientation between allotriomorphic ferrite and bainite variants at the right side of ferrite shown in Fig. 4(b).

Variant	V23	V20	V24	V15	V5	V2	V22	V12	V8	V7	V19
Misorientation	32°	34°	37°	31°	28°	25°	51°	50°	42°	21°	47°

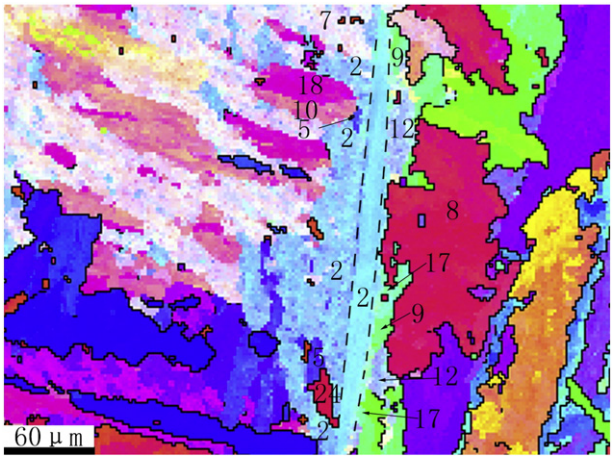

Fig. 6 – Inverse pole figure of the area in Fig. 3(b).

and 6°, respectively. A plate of another variant V8 is also seen in the orientation map. The misorientation angle of this plate with the ferrite is 55° and this plate traversed the whole grain. Thus, it presumably nucleated elsewhere and impinged the ferrite. From these results plates of these three variants presumably nucleated on the ferrite/austenite boundary by sympathetic nucleation [25,26].

3.4. *Potency of nucleation of bainitic ferrite on the surface of ferrite allotriomorph*

In this section the activation energy of nucleation of bainitic plates at the boundary of allotriomorphic ferrite with the matrix austenite is evaluated using a pillbox critical nucleus model. This model was proposed a few decades ago to analyze the nucleation kinetics of proeutectoid ferrite at austenite grain boundary [27]. Hillert [28] reported that carbon is

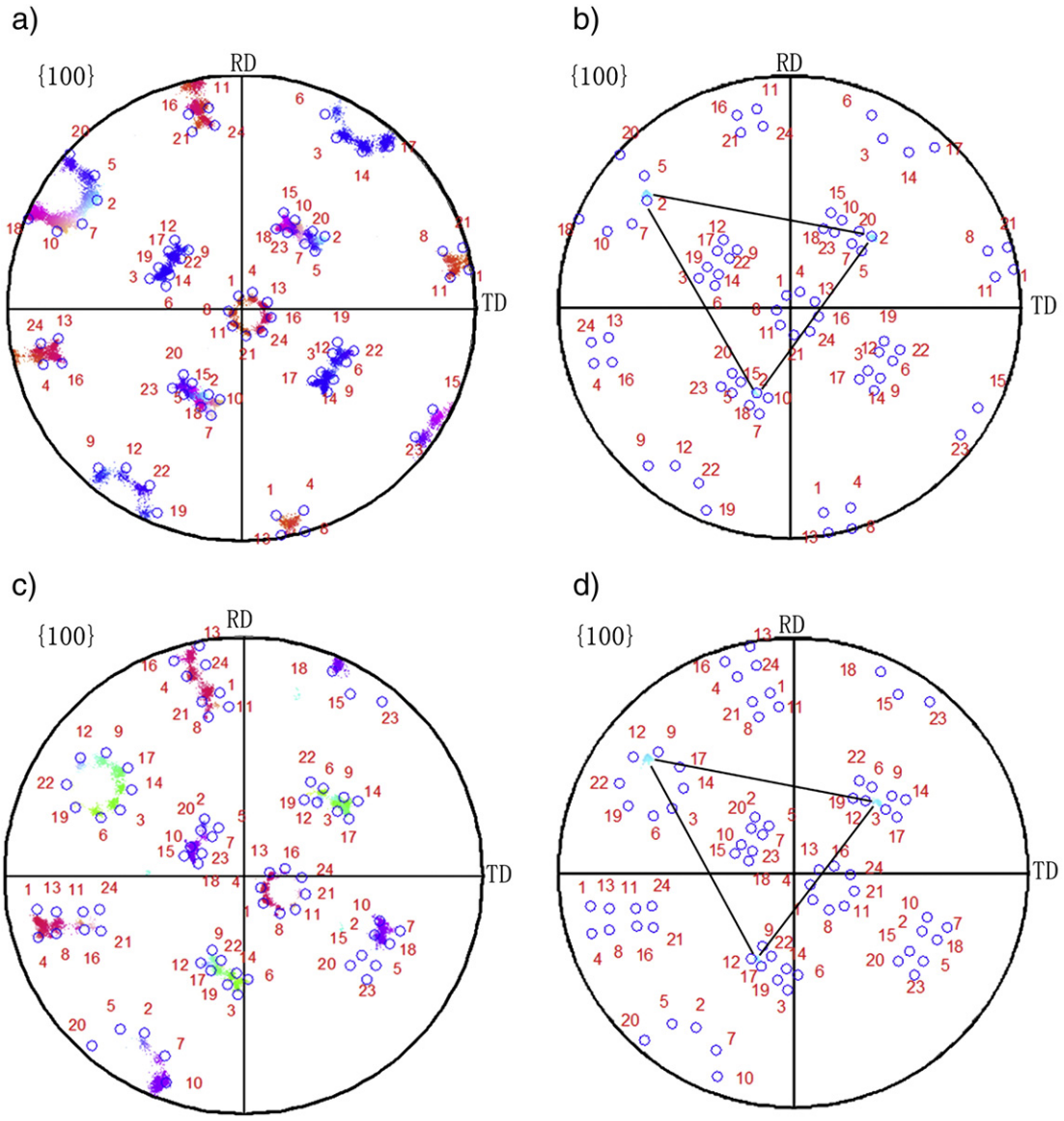

Fig. 7 – {100} pole figures of simulated K-S variants in the left grain of Fig. 6, superimposed by measured orientation of (a) bainite and (b) allotriomorphic ferrite; And {100} pole figures of simulated K-S variants in the right grain of Fig. 6, superimposed by measured orientation of (c) bainite and (d) allotriomorphic ferrite.

partitioned almost to equilibrium during the growth of bainitic plate and thus a bainitic plate can be treated in the same way as Widmanstatten ferrite which forms above the T0 temperature (temperature at which the free energy of ferrite and austenite of the same composition becomes identical). It is thus assumed that the theory of diffusional nucleation is applicable to the nucleation of bainitic plate which occurred in the ($\alpha+\gamma$) two-phase region in this alloy. To begin with, the nucleation on the boundary between K-S oriented allotriomorphic ferrite and austenite is considered. The free energy change attending nucleation can be expressed as [25,26]

$$\Delta G = \pi r^2 h\varphi + \pi r^2\left(A_{\alpha\alpha} + A^{KS}_{\alpha\gamma} - A^{KS\,\prime}_{\alpha\gamma}\right) + 2\pi r h A^{e}_{\alpha\gamma} \quad (1)$$

where ϕ is the sum of the volume free energy change and elastic strain energy of nucleus in front of the K-S oriented boundary, $A_{\alpha\alpha}$ is the interfacial energy between allotriomorphic and bainitic ferrite, $A^{KS}_{\alpha\gamma}$ is the interfacial energy between bainitic ferrite and austenite, $A^{KS}_{\alpha\gamma}$', is the interfacial energy between allotriomorphic ferrite and austenite which extinguished upon nucleation, and $A^{e}_{\alpha\gamma}$ is the edge energy of the pillbox nucleus. Differentiating ΔG with respect to r and h, the activation energy of nucleation can be expressed as [25,27]

$$\Delta G^{*} = 4\pi\left(A^{e}_{\alpha\gamma}\right)^2 \frac{A_{\alpha\alpha} + A^{KS}_{\alpha\gamma} - A^{KS\,\prime}_{\alpha\gamma}}{\varphi^2} \approx 4\pi\left(A^{e}_{\alpha\gamma}\right)^2 \frac{A_{\alpha\alpha}}{\varphi^2} \quad (2)$$

If the nucleation of bainitic ferrite had the same variant with the ferrite allotriomorph, $A^{KS}_{\alpha\gamma}$ and $A^{KS}_{\alpha\gamma}$' values can be similar. Moreover, if it occurred sympathetically on the surface of allotriomorph, the nucleus is thought to have a misorientation of a few degrees with the substrate crystal. Thus, $A_{\alpha\alpha}$ is likely to be less than several tenths of J/m^2 from Read–Shockley equation [29] of the energy of low-angle boundary. The selection of any other 23 variants in the K-S relationship will increase $A_{\alpha\alpha}$, and such a nucleus may be energetically unfavorable.

When bainitic ferrite was nucleated on the boundary which did not have a K-S relationship, the activation energy of nucleation is expressed by,

$$\Delta G'^{*} = 4\pi\left(A^{e}_{\alpha\gamma}\right)^2 \frac{A_{\alpha\alpha} + A^{KS}_{\alpha\gamma} - A^{ir\,\prime}_{\alpha\gamma}}{\varphi'^2} \approx 4\pi\left(A^{e}_{\alpha\gamma}\right)^2 \frac{A^{KS}_{\alpha\gamma}}{\varphi'^2} \quad (3)$$

where ϕ' is the driving force near the irrationally oriented ferrite/austenite boundary and $A^{ir}_{\alpha\gamma}$' is the interfacial energy of such a boundary. $A^{KS}_{\alpha\gamma}$ in the numerator occurs due to the fact that bainitic ferrite plates bear a K-S relationship with the matrix. It was reported that the energy of ferrite/austenite boundary is somewhat smaller (less than several percent) than the ferrite grain boundary energy [30]. If one ignores this difference ($A_{\alpha\alpha} \approx A^{ir}_{\alpha\gamma}$'), Eq. (2) indicates that $A^{KS}_{\alpha\gamma}$ plays a key role in nucleation. The lowest energy of ferrite/austenite boundary having a K-S relationship was calculated to be a few tenths of J/m^2 [31], the same order as $A_{\alpha\alpha}$ in Eq. (2).

According to Hillert (Fig.8 in ref. [28]), the growth of ferrite allotriomorph occurs often by migration of only one boundary. On the moving boundary side carbon diffuses immediately into the matrix whereas carbon diffuses through the ferrite and then into the matrix on the stationery boundary side. Since carbon diffuses on both sides of the moving boundary, the thickness of ferrite allotriomorph becomes similar to that of ferrite allotriomorph of which both boundaries migrate. The carbon build-up does occur, but to a lesser extent on the stationery side due to a larger distance from the moving boundary. Although carbon atoms built up around the allotriomorphic ferrite diffuse away during holding at 725 °C, the driving force in front of the moving irrational boundary ϕ' in Eq. (3) can be considerably smaller than ϕ in Eq. (2). This may indicate that the nucleation potency of K-S oriented allotriomorph boundary is larger than that of irrational boundary if the carbon builds up remains at the 2nd holding temperature.

It is possible that bainitic plate on the right side in Fig. 4b was nucleated within the matrix, e.g. at dislocations etc. If the energy of such defects was ignored, the activation energy of nucleation within the matrix is given by the equation,

$$\Delta G_M^{*} = 4\pi\left(A^{e}_{\alpha\gamma}\right)^2 \frac{2A^{KS}_{\alpha\gamma}}{\varphi_M{}^2} \quad (4)$$

where ϕ_M is the free energy change attending nucleation at the bulk carbon concentration. ΔG^{*}_{M} becomes smaller if one includes the energy of defects which disappear upon nucleation. Since ϕ_M is more negative than ϕ and ϕ', one cannot rule out the possibility that bainitic ferrite plates were nucleated at some defects within the matrix although the numerator of the right hand side of Eq. (4) is greater than those of Eqs. (2) and (3). In this experiment it seems that the activation energy of nucleation of bainite ΔG^{*} is the smallest near the K-S oriented ferrite/austenite boundary and $\Delta G'^{*}$ is greater than ΔG^{*}_{M} from the distribution of K-S variants near the ferrite allotriomorphs.

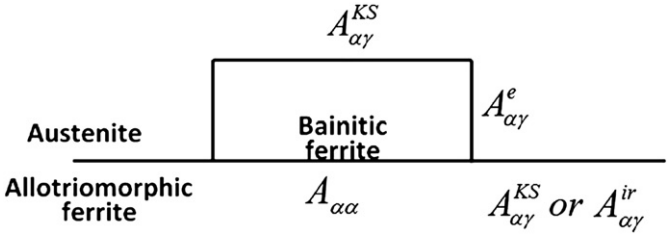

Fig. 8 – Schematic drawings of the pillbox model for critical nuclei at: (a) ferrite/austenite boundary where a K-S relationship is maintained, and (b) at ferrite/austenite boundary where the relative orientation is significantly deviated from the K-S relationship.

4. Summary

The orientation of bainitic plates near the ferrite allotriomorphs was analyzed in a low carbon Fe-0.05C-2.9Mn-1.8Si alloy. About 80% ferrite allotriomorphs maintained a K-S orientation relationship with one of the adjacent austenite grains and about 10% of them exhibited the K-S relationship with both grains. In the austenite grain which had an almost exact K-S relationship with the ferrite (the deviation was less than experimental error of ~1°) bainitic plates selected the same variant as the ferrite allotriomorph. They often covered the whole surface of the allotriomorph, occasionally with another variant that formed a sub-block and had a misorientation angle of 10.5° with the variant of ferrite. In the austenite grain which had an orientation several degrees deviated from the exact K-S relationship, bainitic plates chose the variants that had a small misorientation angle, mostly several degrees, with the ferrite. When the matrix austenite grain had an irrational orientation relationship, no variant selection appeared to occur during nucleation.

These results indicate that nucleation of bainitic plates was enhanced on the surface of allotriomorph when it had a K-S relationship with the matrix grain because the nucleus was able to form a low energy interface with the ferrite. In contrast, the surface of allotriomorph which was irrationally oriented with the matrix grain did not appear to promote nucleation of bainitic plates presumably because a variant of large misorientation with the ferrite was nucleated and a larger amount of carbon was built up near the boundary during the prior isothermal holding.

Acknowledgements

The authors owe thanks to Prof. Wenzheng Zhang and Mr. Fuzhi Dai in the Department of Materials Science and Engineering in Tsinghua University for the help to develop the program to draw <001> poles of K-S variants. This paper is financially supported by the National Nature Science Foundation of China with the contracts of No. 50601002 and No. 50971028.

REFERENCES

[1] Lambert-Perlade A, Gourgues AF, Pineau A. Austenite to bainite phase transformation in the heat-affected zone of a high strength low alloy steel. Acta Mater 2004;52:2337–48.
[2] Furuhara T, Kawata H, Morito S, Maki T. Crystallography of upper bainite in Fe-Ni-C alloys. Mater Sci Eng A 2006;431:228–36.
[3] Kawata H, Sakamoto K, Moritani T, Morito S, Furuhara T, Maki T. Crystallography of ausformed upper bainite structure in Fe-9Ni-C alloys. Mater Sci Eng A 2006;438–40:140–4.
[4] Ohmori Y, Ohtsubo H, Jung YC, Okaguchi S, Ohtani H. Morphology of bainite and Widmanstätten ferrite. Metall Mater Trans A 1994;25A:1981–9.
[5] Hackenberg RE, Shiflet GJ. The influence of morphology on grain-boundary and twin-boundary bainite growth kinetics at the bay in Fe-C-Mo. Phil Mag 2003;83:3367–85.
[6] Furuhara T, Maki T. Variant selection in heterogeneous nucleation on defects in diffusional phase transformation and precipitation. Mater Sci Eng A 2001;312(1–2):145–54.
[7] Quidort D, Brechet YJM. Isothermal growth kinetics of bainite in 0.5% C steels. Acta Mater 2001;49(20):4161–70.
[8] Kim D, Suh DW. Dual orientation and variant selection during diffusional transformation of austenite to allotriomorphic ferrite. J Mater Sci 2010;45(15):4126–32.
[9] Suh DW, et al. Evaluation of the deviation angel of ferrite from the Kurdjumov–Sachs relationship in a low carbon steel by EBSD. Scr Mater 2002;46:375.
[10] Choi JY, et al. Orientation distribution of proeuctectoid ferrite nucleated at prior austenite grain boundaries in vanadium-added steel. ISI Int 2002;42:1321.
[11] Guo H, Purdy GR, Enomoto M, Aaronson HI. Kinetic transitions and substititional solute (Mn) fields associated with later stages of ferrite growth in Fe-C-Mn-Si. Metall Mater Trans A 2006;37A:1721–9.
[12] Andrew KW. Empirical formulae for the calculations of some transformation temperatures. J Iron Steel Inst 1965;203:721–7.
[13] Cui GB, Guo H, Yang SW, He XL. Influence of interface between grain boundary ferrite and prior austenite on bainite transformation in a low carbon steel. Acta Metall Sin 2009;45:680–6.
[14] Guo H. unpublished work, University of Science and Technology Beijing, 2011.
[15] Araki T. Atlas for bainitic microstructures. Continuous-cooled microstructures of low-carbon steels, vol. 1. Tokyo: Iron and Steel Institute of Japan; 1992.
[16] Guo H, Bai Y, Yang SW, He XL. Nucleation of bainite on allotriomorphic ferrite/austenite interface in a low carbon steel. Mater Sci Forum 2010;654–656:2326–9.
[17] King AD, Bell T. Crystallography of grain boundary proeutectoid ferrite. Metall Mater Trans A 1975;7(6A):1419–29.
[18] Ryder PL, Pitsch W, Mehl RF. Crystallography of the precipitation of ferrite on austenite grain boundaries in a Co + 20% Fe alloy. Acta Metall 1967;15:1431–40.
[19] Adachi Y, Hakata K, Tsuzaki K. Crystallographic analysis of grain boundary Bcc-precipitates in a Ni–Cr alloy by FESEM/EBSD and TEM/Kikuchi line methods. Mater Sci Eng A 2005;412:252–63.
[20] Landheer H, Offerman SE, Petrov RH, Kestens LAI. The role of crystal misorientations during solid-state nucleation of ferrite in austenite. Acta Mater 2009;57:1486–96.
[21] Zhang GH, Enomoto M. Metall. Influence of Crystallography on Ferrite Nucleation at Austenite Grain-Boundary Faces, Edges, and Corners in a Co-15Fe Alloy. Metall Mater Trans A 2011;42A:1597–608.
[22] Guo H, Bai Y, Deng Y, Yang SW, He XL. Influence of allotriomorphic ferrite under different growth modes on the variant selection of bainite in a low carbon steel. Adv Mater Res 2012;399–401:200–5.
[23] Smith CS. Microstructure. Trans ASM 1953;45:533–75.
[24] Furuhara T, Kawata H, Morito S, Miyamoto G, Maki T. Variant selection in grain boundary nucleation of upper bainite. Metall Mater Trans 2008;39A:1003–13.
[25] Menon ESK, Aaronson HI. Overview no. 57 morphology, crystallography and kinetics of sympathetic nucleation. Acta Metall 1987;35:549–63.
[26] Aaronson HI, Spanos G, Masamura RA, Vardiman RG, Moon DW, Menon ESK. Sympathetic nucleation: an overview Hall MG. Mater Sci Eng B 1995;32:107–23.
[27] Lang WF, Enomoto M, Aaronson HI. The kinetics of ferrite nucleation at austenite grain boundaries in Fe-C alloys. Metall Mater Trans A 1988;19A:427–40.
[28] Hillert M. Diffusion in growth of bainite. Metall Mater Trans A 1994;25A:1957–66.
[29] Read Jr WT. Dislocations in Crystals. New York: McGraw-Hill; 1953. p. 155–70.
[30] Gjostein NA, Domian HA, Aaronson HI, Eichen E. Relative interfacial energies in Fe-C alloys. Acta Metall 1966;14:1637–44.
[31] Nagano T, Enomoto M. Calculation of the interfacial energies between α and γ iron and equilibrium particle shape. Metall Mater Trans A 2006;37A:929–37.